J Mater Sci (2018) 53:6831–6841

Energy materials

Highly dispersed RuCo bimetallic nanoparticles supported on carbon black: enhanced catalytic activity for hydrogen generation from $NaBH_4$ methanolysis

Fanghui Wang[1], Yanan Wang[1], Yajun Zhang[1], Yimeng Luo[1], and Hong Zhu[1,*]

[1] State Key Laboratory of Chemical Resource Engineering, Institute of Modern Catalysis, Department of Organic Chemistry, School of Science, Beijing University of Chemical Technology, Beijing 100029, People's Republic of China

Received: 19 October 2017
Accepted: 8 January 2018
Published online: 2 February 2018

ABSTRACT

A series of carbon black-supported bimetallic Ru–Co nanoparticles catalyst were synthesized via the chemical reduction of corresponding metal precursor in ethylene glycol, for H_2 generation from $NaBH_4$ methanolysis. The composition, morphology and structure of the novel nanomaterial were well characterized by XRD, XPS, HRTEM, EDX and SEM, showing the good dispersion of supported Ru–Co nanoparticles with an average diameter of 2.4 nm. Significantly, the highest H_2 generation rate is observed in the case of Ru–Co/C catalyst with Ru/Co ratio of 5, achieving 9.36 L min^{-1} g^{-1} at 25 °C, which is comparable to the reported pure Ru catalysts. Furthermore, the recycle test confirms our catalyst can be practically applied. Our work highlights the synergetic effect in bimetallic catalytic system for boosting H_2 generation rates from $NaBH_4$ methanolysis.

Introduction

Due to its gaseous nature and low density at room temperature, storage and transportation of hydrogen are still obstacles to the development of proton exchange membrane fuel cell (PEMFC) [1]. Hence, to solve the problem, the concept of solid hydrogen storage has been proposed and attracted intense attentions [2]. Sodium borohydride ($NaBH_4$) has been considered as a potential candidate for hydrogen storage in the light of its high gravimetric density (10.8 wt%) [3, 4], environmental friendliness and potentially safe operation [5–7]. In 2001, $NaBH_4$, a solid hydrogen storage material, was first successfully applied to Daimler Chrysler's fuel cell concept minivan by Millennium Cell Corporation of American [8, 9].

The generation rates of hydrogen gas can be promoted by introducing a proper catalyst [10–13], such as Co–TiO_2 [14], Ru/Al_2O_3 [15], Fe–B/Ni foam [16], Co/Al_2O_3 [17], Ni_2P/SiO_2 [18], MWCN–COOH [19], polyethyleneimine microgels [20], Hal nanotube [21] and P/boehmite [22]. Among these catalysts, Ru catalyst showed the highest efficiency of catalytic activity compared with other metal catalysts [23–28],

Address correspondence to E-mail: zhuho128@126.com

https://doi.org/10.1007/s10853-018-2013-1

but its practical application was restricted by the expensive price and limited resources. These limitations have inspired many efforts to develop cost-effective non-noble metal (Ni, Fe [29–34] and Co [35–41], etc.) catalysts as an alternative. In the past decades, considerable progress has been achieved in this area, especially in the case of Co-based catalysts. However, it is still far from satisfaction to achieve our goal.

Recently, bimetallic nanoparticles with large surface area and unique role of controlling the selectivity, activity, and stability are found to be more effective than monometallic catalysts in the field of catalysis [42–45]. In view of the above advantages of the bimetallic nanoparticles, in this study, we synthesize supported noble and non-noble bimetallic (Ru–Co) nanoparticles to catalyze H_2 generation from $NaBH_4$ methanolysis (Scheme 1) for the first time. The results illustrated that the as-synthesized Ru–Co bimetallic nanoparticles are uniformly dispersed on the support with an average diameter of 2.4 nm. Besides, hydrogen generation tests also presented that the displayed catalyst significantly enhanced the catalytic activity toward $NaBH_4$ methanolysis, indicating that Ru–Co bimetallic nanoparticles catalyst is a promising candidate to replace pure Ru catalyst in H_2 generation from $NaBH_4$ methanolysis.

Experimental section

Materials

The support material carbon black was purchased from AkzoNobel. The reagents were at the analytical grade without further purification. Ruthenium chloride ($RuCl_3$), cobalt chloride ($CoCl_2{\cdot}6H_2O$), sodium borohydride ($NaBH_4$), methanol (CH_3OH), ethylene glycol (EG) and sodium hydroxide (NaOH) were purchased from Sigma Aldrich.

Preparation of catalysts

In order to get the carboxyl group functionalized carbon black, 2.0 g carbon black was dispersed in 30 wt% HNO_3 aqueous solution and the mixture was then refluxed at 140 °C for 2 h (Scheme 1i). After experiencing the cooling system, the rough carbon black was then acquired by filtering and washed by deionized water. Then the pure carbon black support can be obtained after dried for 12 h in 60 °C oven.

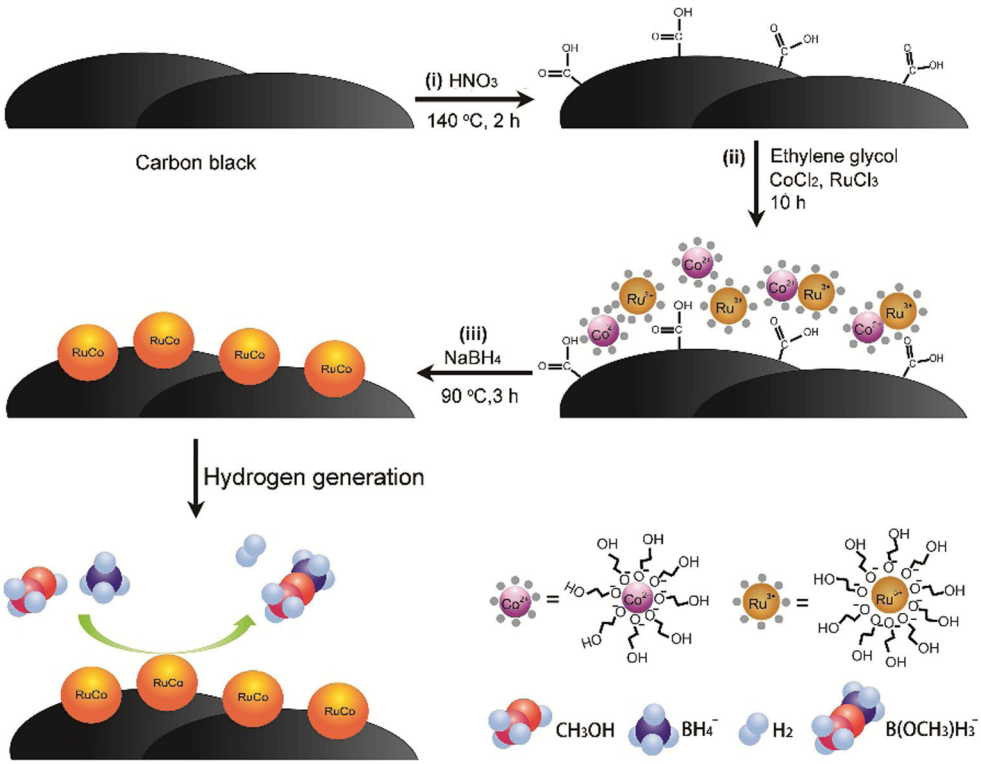

Scheme 1 Preparation of Ru–Co/C bimetallic nanoparticle catalyst.

Carbon-black-supported Ru–Co nanoparticles (Ru–Co/C) were prepared by co-reduction of the precursors of Ru and Co by the addition of $NaBH_4$. 2.05 ml $RuCl_3$/EG (20 g/L) and 2.02 ml $CoCl_2$/EG (20 g/L) and 80 mg functionalized carbon black above were added to ethylene glycol (EG) with string for 10 h (Scheme 1ii). Then, the pH of the solvents was adjusted to 9.5 by adding NaOH/EG solution (2M). Excess amount of $NaBH_4$ were carefully added into the above flask with string vigorously, and the reaction solution was heated at 90 °C for 3 h (Scheme 1iii). After the washing and separating process, the products were dried in the oven at 60 °C for 12 h. Ru–Co nanoparticles with different molar ratio of Ru/Co were prepared by adjusting the molar concentrations of $RuCl_3$ and $CoCl_2$, which were denoted as Ru_xCo_y/C (x/y = molar ratio, when the value of y was 1, it was omitted).

Catalytic activity of Ru–Co/C

A batch-type hydrogen generation system was used to evaluate the catalytic activity of Ru–Co/C nanoparticles. In a typical measurement, the flask was loaded with $NaBH_4$ alkaline methanol solution (20 ml, 10 wt% $NaBH_4$ and 1 wt% NaOH). Twenty micrograms of Ru–Co/C catalyst was introduced to the flask by an injector. The generated hydrogen stream passed through a gas mass flow meter (Sevenstar CS200C) to measure the hydrogen generation rate.

Characterization of catalysts

The structure of carbon black was characterized by Fourier transform infrared radiation spectroscopy (FTIR, Nicolet 6700). The crystallization of Ru–Co/C nanoparticles was characterized by X-ray diffraction (XRD, Shimadzu XD-3A diffractometer) and thermogravimetric analysis (TG, Hengjiu HTG-2). TG was implemented from 40 to 900 °C under O_2 flow. Transmission electron microscope (TEM) tests were measured by JEOL JEM-3010HR. Energy-dispersive X-ray spectroscopy (EDX) was employed to measure the elements composition of catalysts. X-ray photoelectron spectroscopy (XPS) tests were measured by Thermo Fisher LAB 250 ESCA System.

Results and discussion

Characterization of the catalysts

Initially, 37 wt% HCl and 30 wt% HNO_3 are both applied to treat the carbon black. However, only HNO_3-treated carbon black shows obvious changes in the FTIR (Fig. 1a). Compared with the un-treated carbon black, two obvious peaks at 1734.25 and 1210.30 cm^{-1} are attributed to the stretching of carboxyl groups. It is indicated that there are abundant carboxyl groups on the carbon black surface. Furthermore, these carboxyl groups could improve the hydrophilic property and the dispersion of carbon black in the ethylene glycol (EG) solvent. Meanwhile, the exposed carboxyl groups favor the absorption of Ru^{3+} and Co^{2+} precursors on the surface of the carbon black.

The XRD pattern of Ru–Co/C is shown in Fig. 1b. A peak at $2\theta = 25.00°$ can be seen in the spectrum, which can be attributed to the carbon black. Meanwhile, the peak at $2\theta = 44°$ can be interpreted as the (101) plane of ruthenium of amorphous state. Notably, the peak of Co does not appear because of the lower reduction potential of Co^{2+}/Co^0 [37, 38]. To confirm the existence of Co metal, the samples are calcined at 500 °C for 2 h under N_2 atmosphere and the heat-treated Ru–Co/C is characterized by XRD, which is shown in Fig. 1c. Many sharp peaks at $2\theta = 40.00°$, 43.40°, 45.77°, 60.50°, 72.62° and 81.33° in the XRD pattern completely match with the diffraction peaks of the standard Ru–Co alloy (JCPDS 65-8976). Besides the XRD test, TG is carried to measure the total metal loading of Ru–Co/C, as shown in Fig. 1d. Under O_2 flow, carbon black decomposes above 250 °C, but metal compositions are still stable. The final weight of 26.5% indicates the actual metal loading.

In order to further determine the presence of Ru and Co metals, we selected two regions of the primary Ru–Co/C to test the EDX, which are shown in S1(a) and (b) in supplementary information. The EDX results (Table 1) suggest the atomic ratios of Ru to Co are 5.57 and 5.64 in region 1 and region 2, respectively, indicating that the Ru and Co metals exist and distribute uniformly on the carbon black support.

The as-synthesized catalysts are then characterized by the TEM and SEM, and the test results are shown in Fig. 2a, b, e, f. Compared with the previous Ru catalyst prepared in the water solvent [28, 46], our

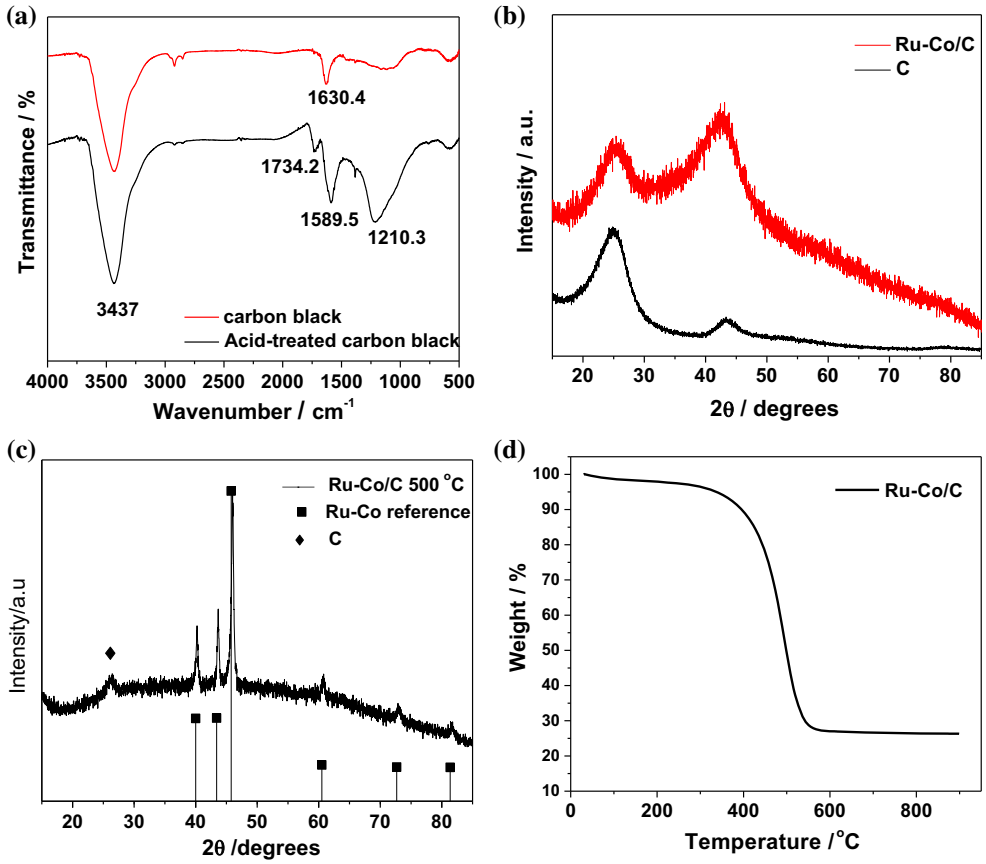

Figure 1 **a** FTIR pattern of carbon black and HNO_3-treated carbon black; **b** XRD pattern of Ru–Co/C and carbon black; **c** XRD pattern of calcined Ru–Co/C at 500 °C and standard diffraction peaks of Ru–Co alloy; **d** TG curve of Ru–Co/C.

Table 1 Element composition of Ru_5Co/C catalyst

Element	Region 1/atom%	Region 2/atom%
Ru	84.77	84.94
Co	15.23	15.06
Ru/Co ratio	5.57	5.64

Ru–Co nanoparticles have a higher dispersion on the carbon surface because the EG solvent reduced the agglomeration of the nanoparticles during the preparing process. Moreover, the average diameters of Ru–Co nanoparticles and Ru nanoparticles are just 2.40 and 4.32 nm, respectively. To further characterize the as-synthesized catalysts, the HRTEM tests are carried out for the catalysts, as shown in Fig. 2. As we can see from Figs. 3c and Fig. 2d, the inter-planar spacing of pure Ru and the Ru–Co nanoparticles nanoparticles is 0.2352 and 0.2123 nm, respectively, which is between the inter-planar spacing of the (100) face of Ru (0.2343 nm; Ru: JCPDS 89-4903) and the (101) face of Co (0.1915 nm; Co: JCPDS 89-7373). The above results illustrate that the Ru and Co are not monometallic nanoparticles on carbon black but alloy-structured nanoparticles.

In order to verify the alloy structure of Ru–Co nanoparticles, XPS was implemented. Figure 3a shows the XPS spectra of each element of the Ru–Co/C catalyst. The C 1*s* spectrum (Fig. 3b) can be fitted by three chemical states at binding energies of 284.8, 286.2 and 289.0 eV, corresponding to C in the form of C–C, C–OH and O=C–OH, respectively. The single peak at 281.5 eV is attributed to Ru 3*d*, which shows a little shift of 0.4 eV compared with that of pure Ru nanoparticles. Ru $3p_{3/2}$ and Ru $3p_{1/2}$ can be assigned to the binding energies of 463.0 and 485.2 eV in Fig. 3c, respectively. For Co (Fig. 3d), the signals at binding energies of 780.10 and 796.85 eV are corresponded to Co $2p_{3/2}$ and Co $2p_{1/2}$ peaks of Co^0, respectively, and binding energies of 786.9 and 802.0 eV are corresponded to Co $2p_{3/2}$ and Co $2p_{1/2}$ peaks of CoO, respectively. The peak at binding

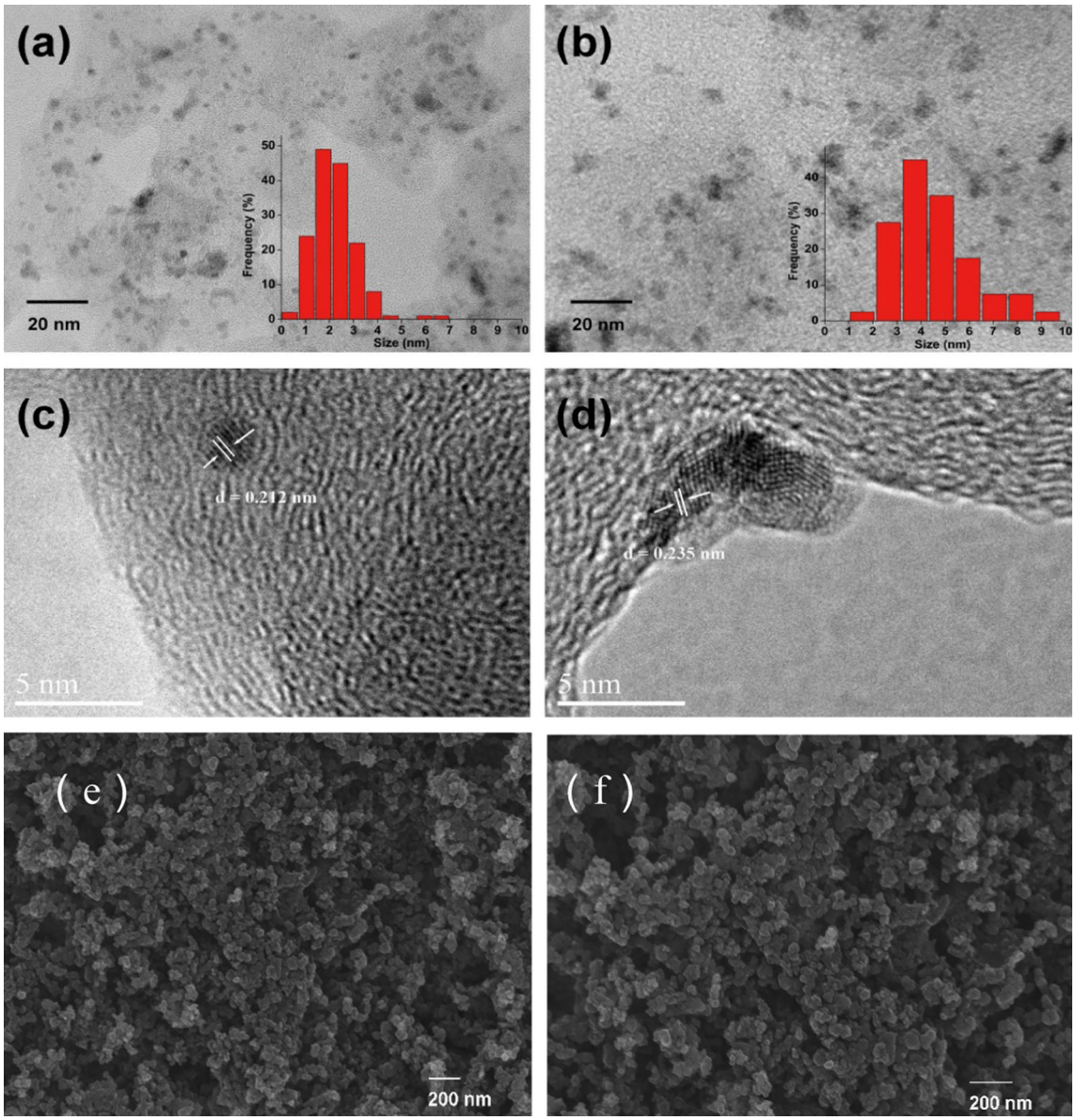

Figure 2 TEM images of **a** Ru–Co/C and **b** Ru/C catalyst; HRTEM images of **c** Ru–Co/C and **d** Ru/C catalyst; SEM images of **e** Ru–Co/C and **f** Ru/C.

energy of 783.6 eV is ascribed to Co $2p_{3/2}$ of $Co(OH)_2$, resulting from the inevitable by-product during catalysts preparation processes [47, 48].

Correlation between catalyst composition, microstructure and catalytic activity

During the methanolysis process, electron transfers between the catalysts, reactants are combined with the active sites on the surface of the catalyst, which is, BH_4^- combines the positively charged metal and CH_3OH combines the negatively charged metal to release a H atom, respectively. Then, two H atoms combine to produce hydrogen. As a result, the hydrogen generation rate depends on the composition of the catalyst, and the concentration of $NaBH_4$ and NaOH in the process of methanolysis of $NaBH_4$. Based on the electronic-structure calculations by Nørskov et al. [49], Ru–Co bimetallic alloy could show better performance than pure Ru in catalyzing hydrogen evolution. Therefore, Ru–Co/C catalysts with the Ru/Co molar ratio of 1:1, 2:1, 3:1, 4:1, 5:1 and 6:1 were prepared and applied to catalyze the H_2 generation from methanolysis of $NaBH_4$ under same

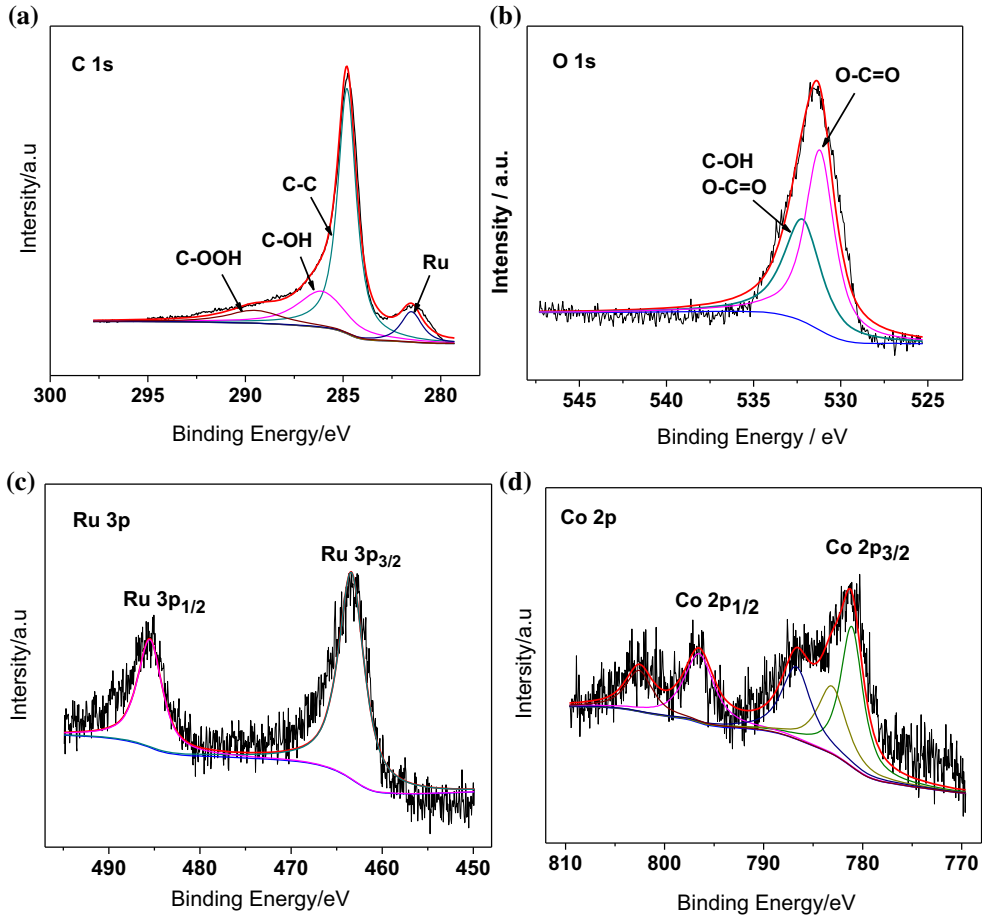

Figure 3 XPS spectra of Ru–Co/C catalyst.

condition (Fig. 4a). The faster the hydrogen generation rate is obtained, the more active the Ru–Co/C catalyst is. The hydrogen generation rate increases with Ru/Co molar ratio on the initial stage, to the maximal rate at the Ru/Co ratio of 5, and then decreases. Ru_3Co/C, Ru_4Co/C, Ru_5Co/C, and Ru_6Co/C all show higher hydrogen generation rate than Ru/C, and the maximum hydrogen generation rate of Ru_5Co/C reaches up to 9.36 L min^{-1} g^{-1}, which is 54.4% higher than Ru/C. Here, this phenomenon can be explained by the Sabatier principle, only the catalyst surface with optimal binding energy of intermediate can achieve the best catalyst activity [50]. In other words, low intermediates binding energies of the catalyst could not trigger the reaction, in contrast, high binding energies would prevent the product dissociating from the catalyst surface [24]. On the other hand, the Ru–Co/C catalysts show enhanced activity due to the small size and the high dispersion of the nanoparticles, which leads to a larger specific surface area than Ru/C catalyst [45]. Furthermore, BET data (Table 2) was implemented to support this point. Hence, the Ru–Co/C catalyst with an optimal Ru/Co molar ratio (Ru_5Co/C) presents the best catalyst performance to generate H_2 from $NaBH_4$ methanolysis.

Correlation between reaction conditions and catalytic behavior

Considering that the catalytic performances closely depending on the concentration of $NaBH_4$, the effects of $NaBH_4$ concentration on the H_2 generation rate are investigated using Ru_5Co/C as the catalyst, which is shown in Fig. 4b. It can be seen that the hydrogen generation rate is accelerated with increasing $NaBH_4$ concentration from 5 to 10 wt%. However, further increasing the $NaBH_4$ concentration (15 and 20 wt%) led to the significant decreasing of H_2 generation rate. The average H_2 generation rate of 2.25 L min^{-1} g^{-1} is achieved with the $NaBH_4$ concentration of 10 wt%. These phenomena are consistent with the previous

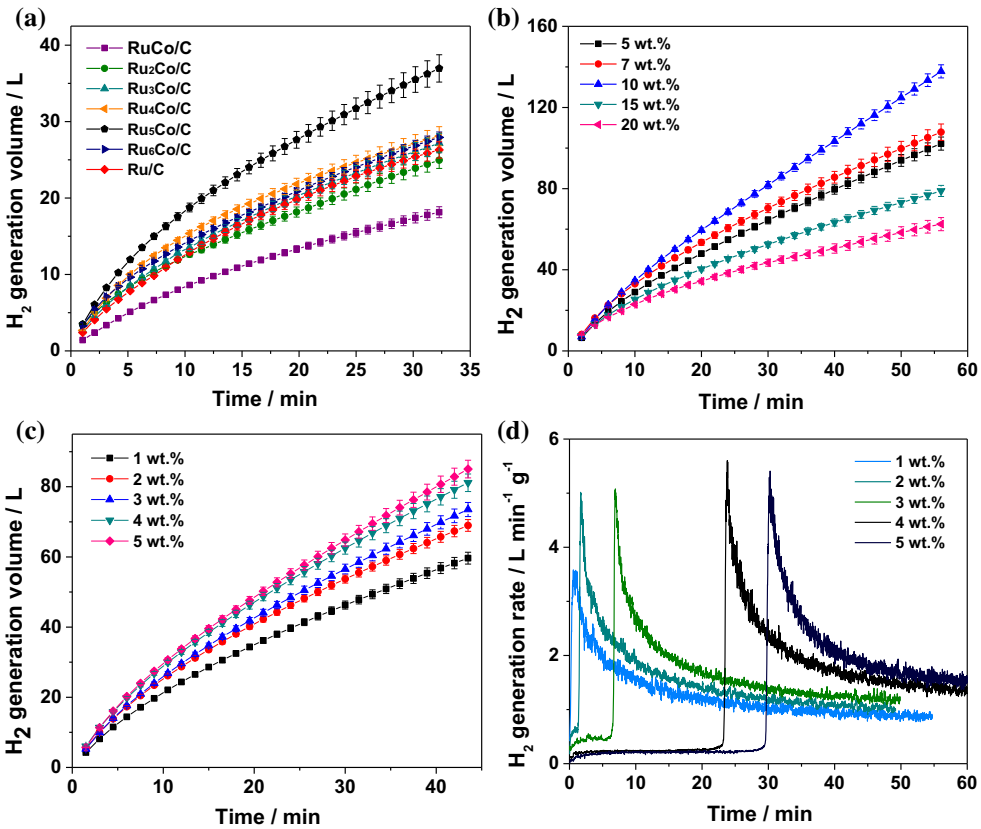

Figure 4 **a** Effect of Ru/Co molar ratio on hydrogen generation (c_{NaBH_4} = 10 wt%, c_{NaOH} = 1 wt%, T = 25 °C); **b** effect of $NaBH_4$ concentration on hydrogen generation (c_{NaOH} = 1 wt%, T = 25 °C, Ru_5Co/C); **c** effect of NaOH concentration on hydrogen generation (c_{NaBH_4} = 10 wt%, T = 25 °C, Ru_5Co/C); **d** effect of NaOH concentration on initial lag time.

Table 2 BET surface area of samples

Samples	Surface area (m^2/g)
Ru/C	289.227
Ru_5Co/C	324.815

results of Patel et al. [36]. and Liang et al. [28]. The above phenomena are attributed to the $NaBH_4$ methanolysis. In fact, the $NaBH_4$ methanolysis process includes the adsorption of BH_4^- on catalyst surface and the reaction of BH_4^- with solvent. At a low $NaBH_4$ concentration, the adsorption of BH_4^- on catalyst surface is the leading role, which caused that the H_2 generation rate increases with $NaBH_4$ concentration increasing. However, at a high $NaBH_4$ concentration, the BH_4^- is saturated on the active sites of catalyst surface so that the reaction of BH_4^- with solvent became the key step. In this situation, the excess BH_4^- causes a considerable solution viscosity, which could limit the mass transport and reduce the methanolysis efficiency [36].

Apart from the effects of $NaBH_4$ concentrations, hydrogen generation experiments are carried out with various concentrations of NaOH solutions. The results (Fig. 4c) show that the average hydrogen generation rate increases from 1.14 to 1.91 L min^{-1} - g^{-1} as the concentration of NaOH rises from 1 to 5 wt%, which means the activity of the Ru–Co/C is weakly dependent on the concentration of NaOH. On the other hand, the initial lag time rises from 1 s to 30 min (Fig. 4d) when the NaOH concentration increases from 1 to 5 wt% because of the inhibiting effect of OH^- anions, which indicates that NaOH could act as a stabilizer in the methanolysis [36]. Much more OH^- anions exist in the high concentration of NaOH, and these OH^- anions will compete with the BH_4^- anions for occupation on the surfaces of the catalyst.

Kinetic study of the catalyzed methanolysis

Kinetic studies at various temperatures in the methanolysis of $NaBH_4$ are carried out. The effects of temperature on the H_2 generation rate with Ru_5Co/C catalyst at the different temperatures are investigated, and the result is shown in Fig. 5a. As expected, H_2 generation rate increases with the increase of the temperature. The hydrogen generation rate of $NaBH_4$

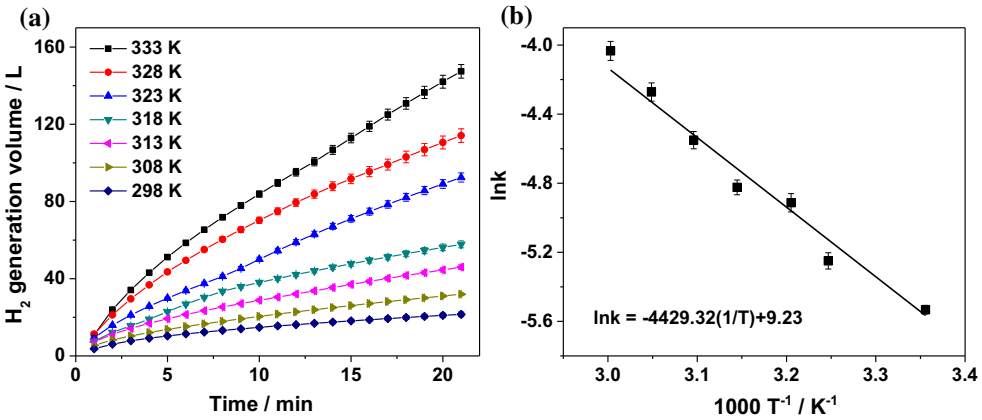

Figure 5 **a** Effect of temperature on hydrogen generation; **b** Arrhenius plot obtained from data in **a** for hydrogen generation from $NaBH_4$ solution.

methanolysis with catalyst can be described by an Arrhenius relation (Eq. 1):

$$r = k_r = A \cdot \exp(-E_a/RT) \quad (1)$$

where r is the reaction rate (mol min^{-1} g^{-1}), A is the reaction constant (mol min^{-1} g^{-1}), E_a is the reaction activation energy (kJ mol^{-1}), R is the gas constant and T is the reaction temperature (K).

From the slope of $\ln k_r$ versus $1/T$ (Fig. 5b), the apparent activation energy (E_a) was determined to be 36.83 kJ mol^{-1}, which is obviously lower than the reported values of $NaBH_4$ spontaneous methanolysis (53.0 kJ mol^{-1} by Lo et al. [51], and 63.0 kJ mol^{-1} by Xu et al. [17]) and value of $NaBH_4$ methanolysis using pure Ru supported on Al_2O_3 as the catalyst (51.0 kJ mol^{-1} by Su et al. [15]).

Reusability of the catalyst

The stability of a catalyst is vital for its application. Figure 6a shows the deterioration in catalytic activity of Ru–Co/C catalyst after reusing the catalyst. The hydrogen yield was calculated by Eq. 2:

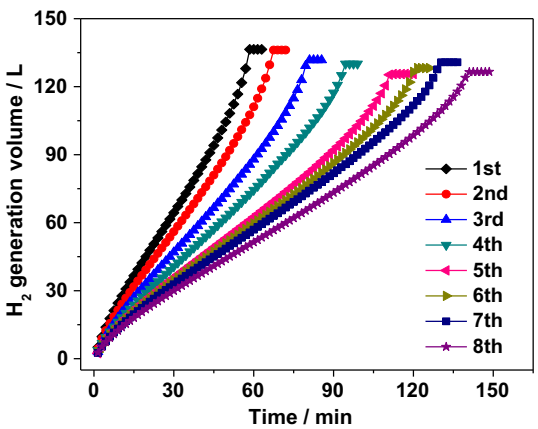

Figure 6 Hydrogen generation in multi-cycle test.

$$\text{Yield}(\%) = \left(\frac{V_r}{V_t}\right) \times 100\% \quad (2)$$

where V_t is the theoretical volume of H_2 generation and V_r is the real volume of H_2 generation [15].

As shown in Fig. 6, the hydrogen yield in the 1st cycle and the 8th cycle are 99.2 and 95.6%, respectively, which indicates the recyclability of catalyst is excellent. In addition, the hydrogen generation rate decreases by 30% after eight cycles. The decrease in efficiency is attributed to the changes of the catalyst composition and the partial inactivation of the catalyst on the surface of by the $NaB(OCH_3)_4$ formation during the reaction.

To test the composition of the catalyst before and after the experiment, the final catalyst was then characterized by the EDX (S2 in supplementary information). The atomic ratio of Ru to Co became 6.43 after eight cycles (Table 3), while the initial ratio was 5.64 before the experiment. This result is in accord with our preceding work (as shown in Fig. 1e, f) which shows that Ru_6Co/C has a lower activity than Ru_5Co/C. The interesting result indicates that the Ru and Co metals still exist on the carbon support. However, part of Co metal was lost from the catalyst caused by erosion of the OH^- in the reaction.

The efficiency of our Ru–Co/C catalysts and the catalysts reported in previous literature are listed in Table 4. Compared to the reported catalysts, the efficiency of our catalysts is far better than that of

Table 3 Element composition of Ru–Co/C catalyst after 8 cycles

Element	Atom%
Ru	86.54
Co	13.46
Ru/Co ratio	6.43

Table 4 Comparison of the maximum H_2 generation rates of the $NaBH_4$ methanolysis between our Ru–Co/C catalyst and various catalysts reported in literature

Catalyst type	$NaBH_4$ (wt%)	NaOH (wt%)	Max rate (L min^{-1} g^{-1})	T (°C)	References
Ru/Al_2O_3	10	1	0.066	25	[15]
Co/Al_2O_3	6	0	0.042	0	[17]
Fe-B	20	1	0.618	25	[18]
Ni_2P	1	0	3.7	25	[22]
Ru/C	10	1	6.06	25	This work
Ru_5Co/C	10	1	9.36	25	This work

many other catalysts including pure Ru/Al_2O_3 catalyst. It should be pointed out that the maximum H_2 generation rates of our catalyst could even reach up to 9.36 L min^{-1} g^{-1}.

Conclusions

In summary, Ru–Co bimetallic nanoparticles supported on the carbon black (Ru–Co/C) have been prepared by the co-reduction method using $NaBH_4$ as a reductant. The average diameter of the Ru–Co nanoparticles is mere 2.4 nm, and the nanoparticles are uniformly dispersed on the carbon black. The materials show an excellent catalytic performance for the H_2 generation from $NaBH_4$ methanolysis. And the maximum H_2 generation rate of the as-synthesized Ru–Co bimetallic nanoparticles at 25 °C could reach up to 9.36 L min^{-1} g^{-1}, which exceeds the values of Ru/C catalyst and most reported values of transition metal or noble metal contained catalysts performed on similar conditions. Due to the synergistic effect of alloyed structure and the smaller average nanoparticles size, the activity of the Ru–Co/C catalysts was greatly enhanced. The Arrhenius apparent activation energy is determined to be 36.83 kJ mol^{-1}, which is significant lower than the values of other catalysts reported in the literature for $NaBH_4$ methanolysis. Besides the high activity, the Ru–Co/C catalysts also exhibit excellent stability and reusability. Though the hydrogen generation rate reduces gradually, the hydrogen yield has no significant decrease after 8 cycles. The results in this study have indicated that the bimetal Ru–Co catalysts can be a relative low-cost and high efficiency catalyst for the substitution of noble metal catalysts in H_2 generation from $NaBH_4$ methanolysis and have potential application in the field of fuel cell.

Acknowledgements

The authors gratefully acknowledge the financial supports from National Natural Science Foundation of China (No. 21476020 and No. 21376022), the National Key Research and Development Program of China (Program No. 2016YFB0101200 (2016YFB0101203)) and Changjiang Scholars and Innovative Research Team in University (IRT1205).

Electronic supplementary material: The online version of this article (https://doi.org/10.1007/s10853-018-2013-1) contains supplementary material, which is available to authorized users.

References

[1] Müller K, Arlt W (2013) Status and development in hydrogen transport and storage for energy applications. Energy Technol 1:501–511

[2] Alebrook AF, Gan WJ, Grasemann M, Moret S, Laurenczy G (2013) Hydrogen storage: beyond conventional methods. Chem Commun (Camb) 49:8735–8751

[3] Louis S, Andreas Z (2001) Hydrogen-storage materials for mobile applications. Nature 414:353–358

[4] Demirci UB, Miele P (2009) Sodium borohydride versus ammonia borane, in hydrogen storage and direct fuel cell applications. Energy Environ Sci 2:627–637

[5] Davis RE, Gottbrath JA (1961) Boron hydrides. V. Methanolysis of sodium borohydride. J Am Chem Soc 84:895–898

[6] Schlesinger HI, Brown HC, Finholt AE, Gilbreath JR, Hoekstra HR (1952) Sodium borohydride, its hydrolysis and its use as a reducing agent and in the generation of hydrogen. J Am Chem Soc 75:215–219

[7] Moussa G, Moury R, Demirci UB, Şener T, Miele P (2013) Boron-based hydrides for chemical hydrogen storage. Int J Energy Res 37:825–842

[8] Amendola SC, Sharp-Goldman SL, Janjua MS, Kelly MT, Petillo PJ, Binder M (2000) An ultrasafe hydrogen generator: aqueous, alkaline borohydride solutions and Ru catalyst. J Power Sources 85:186–189

[9] Zhang JS, Delgass WN, Fisher TS, Gore JP (2007) Kinetics of Ru-catalyzed sodium borohydride hydrolysis. J Power Sources 164:772–781

[10] Zhang QL, Wu Y, Sun XL, Ortega J (2007) Kinetics of catalytic hydrolysis of stabilized sodium borohydride solutions. Ind Eng Chem Res 46:1120–1124

[11] Sahiner N, Senge SB (2016) Quaternized polymeric microgels as metal free catalyst for H2 production from the methanolysis of sodium borohydride. J Power Sources 336:27–34

[12] Sahiner N, Demirci S (2017) Natural microgranular cellulose as alternative catalyst to metal nanoparticles for H_2 production from $NaBH_4$ methanolysis. Appl Catal B Environ 202:199–206

[13] Ramya K, Dhathathreyan KS, Sreenivas J, Kumar S, Narasimhan S (2013) Hydrogen production by alcoholysis of sodium borohydride. Int J Energy Res 37:1889–1895

[14] Hannauer J, Demirci UB, Pastor G, Geantet C, Herrmannb JM, Miele P (2010) Hydrogen release through catalyzed methanolysis of solid sodium borohydride. Energy Environ Sci 3:1796–1803

[15] Su CC, Lu MC, Wang SL, Huang YH (2012) Ruthenium immobilized on Al_2O_3 pellets as a catalyst for hydrogen generation from hydrolysis and methanolysis of sodium borohydride. RSC Adv 2:2073–2079

[16] Ocon JD, Tuan TN, Yi Y, Leon RL, Lee JK, Lee J (2013) Ultrafast and stable hydrogen generation from sodium borohydride in methanol and water over Fe–B nanoparticles. J Power Sources 243:444–450

[17] Xu DY, Zhao L, Dai P, Ji SF (2012) Hydrogen generation from methanolysis of sodium borohydride over Co/Al_2O_3 catalyst. J Nat Gas Chem 21:488–494

[18] Yan KQ, Li YH, Zhang X, Yang X, Zhang NW, Zheng JB, Chen BH, Smith KJ (2015) Effect of preparation method on Ni_2P/SiO_2 catalytic activity for $NaBH_4$ methanolysis and phenol hydrodeoxygenation. Int J Hydrogen Energy 40:16137–16146

[19] Sahiner Nurettin (2017) Modified multi-wall carbon nanotubes as metal free catalyst for application in H_2 production from methanolysis of $NaBH_4$. J Power Sources 366:178–184

[20] Sahiner Nurettin, Demirci Sahin (2017) Very fast H_2 production from the methanolysis of $NaBH_4$ by metal-free poly(ethylene imine) microgel catalysts. Int J Energy Res 41:736–746

[21] Sahinera Nurettin, Sengel Sultan B (2017) Various amine functionalized halloysite nanotube as efficient metal free catalysts for H_2 generation from sodium borohydride methanolysis. Appl Clay Sci 146:517–525

[22] Xu DY, Zhang YS, Cheng F, Zhao L (2014) Enhanced hydrogen generation by methanolysis of sodium borohydride in the presence of phosphorus modified boehmite. Fuel 134:257–262

[23] Zahmakiran M, Özkar S (2008) Intrazeolite ruthenium(0) nanoclusters: a superb catalyst for the hydrogenation of benzene and the hydrolysis of sodium borohydride. Langmuir 24:7065–7067

[24] Demirci UB, Garin F (2008) Ru-based bimetallic alloys for hydrogen generation by hydrolysis of sodium tetrahydroborate. J Alloys Compd 463:107–111

[25] Ferreira MJF, Fernandes VR, Gales L, Rangel CM, Pinto AMFR (2010) Effects of the addition of an organic polymer on the hydrolysis of sodium tetrahydroborate in batch reactors. Int J Hydrogen Energy 35:11456–11469

[26] Li X, Fan G, Zeng C (2014) Synthesis of ruthenium nanoparticles deposited on graphene-like transition metal carbide as an effective catalyst for the hydrolysis of sodium borohydride. Int J Hydrogen Energy 39:14927–14934

[27] Li Y, Zhang Q, Zhang N, Zhu L, Zheng J, Chen BH (2013) $Ru–RuO_2/C$ as an efficient catalyst for the sodium borohydride hydrolysis to hydrogen. Int J Hydrogen Energy 38:13360–13367

[28] Liang Y, Dai HB, Ma LP, Wang P, Cheng HM (2010) Hydrogen generation from sodium borohydride solution using a ruthenium supported on graphite catalyst. Int J Hydrogen Energy 35:3023–3028

[29] Liang Y, Wang P, Dai HB (2010) Hydrogen bubbles dynamic template preparation of a porous Fe–Co–B/Ni foam catalyst for hydrogen generation from hydrolysis of alkaline sodium. J Alloys Compd 491:359–365

[30] Walter JC, Zurawski A, Montgomery D, Thornburg M, Revankar S (2008) Sodium borohydride hydrolysis kinetics comparison for nickel, cobalt, and ruthenium boride catalysts. J Power Sources 179:335–339

[31] Bhattacharjee D, Dasgupta S (2015) Trimetallic NiFePd nanoalloy catalysed hydrogen generation from alkaline hydrous hydrazine and sodium borohydride at room temperature. J Mater Chem A 3:24371–24378

[32] Mori K, Taga T, Yamashita H (2015) Synthesis of a Fe–Ni alloy on a ceria support as a noble-metal-free catalyst for hydrogen production from chemical hydrogen storage materials. ChemCatChem 7:1285–1291

[33] Kılınç Dilek, Şahin Ömer, Saka Cafer (2017) Investigation on salisylaldimine-Ni complex catalyst as an alternative to increasing the performance of catalytic hydrolysis of sodium borohydride. Int J Hydrogen Energy 42:20625–20637

[34] Şahin Ömer, Kılınç Dilek, Saka Cafer (2016) Bimetallic Co–Ni based complex catalyst for hydrogen production by catalytic hydrolysis of sodium borohydride with an alternative approach. J Energy Inst 89:617–626

[35] Şahin Ömer, Kılınç Dilek, Saka Cafer (2016) Hydrogen generation from hydrolysis of sodium borohydride with a novel palladium metal complex catalyst. J Energy Inst 89:182–189

[36] Patel N, Miotello A (2015) Progress in Co–B related catalyst for hydrogen production by hydrolysis of boron-hydrides: a review and the perspectives to substitute noble metals. Int J Hydrogen Energy 40:1429–1464

[37] Patel N, Fernandes R, Miotello A (2009) Hydrogen generation by hydrolysis of $NaBH_4$ with efficient Co–P–B catalyst: a kinetic study. J Power Sources 188:411–420

[38] Arzac GM, Rojas TC, Fernández A (2011) Boron compounds as stabilizers of a complex microstructure in a Co–B-based catalyst for $NaBH_4$ hydrolysis. ChemCatChem 3:1305–1313

[39] Wang LN, Li Z, Liu X, Zhang PP, Xie GW (2015) Hydrogen generation from alkaline $NaBH_4$ solution using electroless-deposited Co-W-P supported on γ-Al_2O_3. Int J Hydrogen Energy 40:7965–7973

[40] Loghmani MH, Shojaei AF (2015) Reduction of cobalt ion improved by lanthanum and zirconium as a triphenylphosphine stabilized nano catalyst for hydrolysis of sodium borohydride. Int J Hydrogen Energy 40:6573–6581

[41] Kılınç Dilek, Saka Cafer, Şahin Ömer (2012) Hydrogen generation from catalytic hydrolysis of sodium borohydride by a novel Co(II)–Cu(II) based complex catalyst. J Power Sources 217:256–261

[42] Wang X, Stöver J, Zielasek V, Altmann L, Karsten T, Al-Shamery K, Bäumer M, Borchert H, Parisi J, Kolny-Olesiak J (2011) Colloidal synthesis and structural control of PtSn bimetallic nanoparticles. Langmuir 27:11052–11061

[43] Jiao C, Huang Z, Wang X, Zhang H, Lu L, Zhang S (2015) Synthesis of Ni/Au/Co trimetallic nanoparticles and their catalytic activity for hydrogen generation from alkaline sodium borohydride aqueous solution. RSC Adv 5:34364–34371

[44] Singh AK, Xu Q (2013) Synergistic catalysis over bimetallic alloy nanoparticles. ChemCatChem 5:652–676

[45] Ai L, Liu X, Jiang J (2016) Synthesis of loofah sponge carbon supported bimetallic silver–cobalt nanoparticles with enhanced catalytic activity towards hydrogen generation from sodium borohydride hydrolysis. J Alloys Compd 625:164–170

[46] Zahmakıran M, Özkar S (2006) Water dispersible acetate stabilized ruthenium(0) nanoclusters as catalyst for hydrogen generation from the hydrolysis of sodium borohyride. J Power Sources 258:95–103

[47] Demirci UB, Miele P (2010) Cobalt in $NaBH_4$ hydrolysis. Phys Chem Chem Phys 12:14651–14655

[48] Inokawa H, Driss H, Trovela F, Miyaoka H, Ichikawa T, Kojima Y (2016) Catalytic hydrolysis of sodium borohydride on Co catalysts. Int J Energy Res 40:2078–2090

[49] Greeley J, Jaramillo TF, Bonde J, Chorkendorff I, Nørskov JK (2006) Computational high-throughput screening of electrocatalytic materials for hydrogen evolution. Nat Mater 5:909–913

[50] Sun D, Mazumder V, Metin Ö, Sun S (2011) Catalytic hydrolysis of ammonia borane via cobalt palladium nanoparticles. ACS Nano 5:6458–6464

[51] Lo CT, Karan K, Davis BR (2007) Kinetic studies of reaction between sodium borohydride and methanol, water, and their mixtures. Ind Eng Chem Res 46:5478–5484